



Contents lists available at ScienceDirect

## Sensors and Actuators: B. Chemical

journal homepage: [www.elsevier.com/locate/snb](http://www.elsevier.com/locate/snb)

# Nanomechanical bio-sensing for fast and reliable detection of viability and susceptibility of microorganisms

Leonardo Venturelli<sup>a,1</sup>, Zoe R. Harrold<sup>b,1</sup>, Alison E. Murray<sup>b</sup>, Maria I. Villalba<sup>c</sup>,  
Eric M. Lundin<sup>b</sup>, Giovanni Dietler<sup>a</sup>, Sandor Kasas<sup>c,d,\*</sup>, Raphael Foschia<sup>a,\*\*</sup>

<sup>a</sup> Laboratory of the Physics of Living Matter, Ecole Polytechnique Fédérale de Lausanne (EPFL), CH-1015 Lausanne, Switzerland

<sup>b</sup> Division of Earth and Ecosystem Sciences, Desert Research Institute, Reno, NV 89512, USA

<sup>c</sup> Laboratory of Biological Electron Microscopy, Ecole Polytechnique Fédérale de Lausanne (EPFL), CH-1015 Lausanne, Switzerland

<sup>d</sup> Unité Facultaire d'Anatomie et de Morphologie (UFAM), CUMRL, Université de Lausanne, CH-1005 Lausanne, Switzerland

## ABSTRACT

The metabolic activity of living organisms results in cellular motion on a nanometric scale that can be efficiently detected by micro- and nano-fabricated sensors. Quartz crystal microbalance and atomic force microscopy (AFM) inspired techniques have recently demonstrated their ability to successfully measure the nanometric motion of microorganisms. Monitoring these fluctuations while exposing the microorganisms to various compounds (e.g., metabolic inhibitors and drugs, fixatives, etc.) provides a rapid, label-free assessment of cellular activity and the live versus dead state of both prokaryotic and eukaryotic cells. To date, microbial activity-induced nanometric oscillations of AFM cantilevers have primarily been measured using commercially available AFMs. In this article we present a novel, user-friendly mechano-sensing device, termed a Nanomotion Detector (NMD), recently developed in our laboratories, that simplifies AFM systems. This NMD offers a streamlined design that is simple to align, is optimized for assays with live cells and liquid exchange, and can be operated in a Peltier-controlled incubator providing thermal control. Here, we successfully tested the ability of the NMD to discern differences between the live/dead nanometric motion of *Escherichia coli* and *Staphylococcus aureus* exposed to antibiotics and fixatives. This NMD is a dedicated cell activity detector that can advantageously replace commercially available AFMs for nanomotion detection applications including rapid antibiotic sensitivity testing.

## 1. Introduction

All living organisms exhibit motion at the nano-scale - or nanomotion - that is above and beyond the frequency of Brownian motion such that it can be considered a universal signal of cellular life. Cellular nanomotion can be efficiently detected and monitored by micro- and nano-fabricated sensors ([17,18,28,32]) regardless of cellular motility. Among others, quartz crystal microbalance [4,24,31] and atomic force microscopy (AFM)-inspired techniques [5,21] have demonstrated their ability to measure extremely sensitive changes in mass and the metabolically-induced oscillations of microorganisms [7,16]. Cellular nanomotion detection techniques eliminate the need for chemical labeling, which can enhance the understanding of cellular physiology by removing biases associated with targeting specific metabolic processes, biochemistry, or cell types and species [6,14]. The measurement of metabolic process or change in mass was indeed demonstrated by Alsteens and colleagues in 2017, opening a new field in living organism nanomotion [2]. Both biomedical and environmental applications can

benefit from nanomotion assays that assess microbial metabolic activity and enable life detection at the cellular scale [10,20]. For example, monitoring nanomotion oscillations while exposing an experimental target organism to various metabolic or cell inhibitors, such as antibiotics or fixatives, provides a measurement of active (live) versus inactive (dead) metabolic states in prokaryotes and eukaryotes [15]. In environmental applications, exposing cells to environmental changes, such as toxins or nutrients, can provide an indication of the limits of life [33].

Nanomotion-based live/dead testing is particularly promising as diagnostic tool for performing rapid antibiotic susceptibility tests (AST), in the medical field [11]. Traditional cell-culture based ASTs are the gold standard used in clinics to determine the most appropriate antibiotic to fight infections [9,27]. Unfortunately, obtaining positive results via traditional ASTs requires between 24 h and three weeks depending on the reproduction rate of the infecting bacteria [3]. Since infections such as sepsis can lead to patient death within hours, clinicians tend to prescribe broad spectrum antibiotics before obtaining the AST results [8]. The primary downfall of the widespread use and misuse of broad

\* Corresponding author at: Laboratory of Biological Electron Microscopy, Ecole Polytechnique Fédérale de Lausanne (EPFL), CH-1015 Lausanne, Switzerland.

\*\* Corresponding author.

E-mail addresses: [sandor.kasas@epfl.ch](mailto:sandor.kasas@epfl.ch) (S. Kasas), [raphael.foschia@hesge.ch](mailto:raphael.foschia@hesge.ch) (R. Foschia).

<sup>1</sup> These authors contributed equally.

<https://doi.org/10.1016/j.snb.2021.130650>

Received 11 May 2021; Received in revised form 14 August 2021; Accepted 23 August 2021

Available online 27 August 2021

0925-4005/© 2021 The Author(s).

Published by Elsevier B.V. This is an open access article under the CC BY-NC-ND license

(<http://creativecommons.org/licenses/by-nc-nd/4.0/>).

spectrum antibiotics is that they have led to bacterial antibiotic resistance, which has been identified as a global public health challenge for the coming decades [1]. Novel assays that reduce the AST time to minutes or hours could dramatically shorten the turnaround time for determining and subsequently prescribing the most efficient, targeted antibiotic needed to fight a given bacterial infection and ultimately reduce reliance on large spectrum antibiotics [3].

Nanomotion detection provides a rapid, label-free, agnostic and unbiased approach to measuring the impact of stressors (e.g. chemicals such as antibiotics, fixatives, etc.) on cellular metabolism and serves as a robust live/dead assay. In 2013, Longo and colleagues demonstrated the ability to record nanomotion in a relatively simple manner by attaching microorganisms onto AFM cantilevers [19] and monitoring the oscillations of the cantilever by capturing laser deflections using a conventional AFM. They showed that the cantilever oscillations decreased after exposing the attached microbes to antibiotics or other cell inactivation agents. Following this initial work several studies have demonstrated nanomotion experiments on a range of living organisms such as yeast [13], mycobacteria [23], *Bordetella pertussis* [30], neurons [25], osteoblasts [12], and cancer cells [29]. This work has just scratched the surface of cellular nanomotion applications due in part to a lack of access to nanomotion detection technology, including dedicated and optimized nanomotion detection instrumentation.

Given the growing applications for measuring cellular activity via nanomotion detection, including in AST applications, there is an increasing need for accessible instrumentation specifically engineered to reliably measure cellular nanomotion.

Here, we present a novel, streamlined nanomotion detector (NMD) specially designed to perform rapid ASTs and advance our understanding of microbial cell activity. This design supports liquid exchange which is an asset for living cell assays. It is also small enough to operate inside a low-vibration, Peltier-cooled/heated incubator which enables precise temperature-controlled experimentation above or below ambient temperatures. The NMD was designed to require minimum adjustments during setup and use, and is unaffected by changes in optical refraction index associated with liquid exchange inside the sample chamber. The device was also fabricated with low-cost materials enhancing the potential for technology transfer. These developments will facilitate broad implementation of the device in medical centers and research laboratories. This work describes the NMD design and demonstrates the ability to detect *Escherichia coli* and *Staphylococcus aureus* nanomotion under temperature-controlled conditions and conduct rapid and reliable ASTs.

## 2. Methods

### 2.1. Elements of nanomotion detector design

The NMD was designed, machined, assembled, and tested in the laboratory of physics of living matter at the *Ecole Polytechnique Fédérale de Lausanne* (EPFL, Switzerland). The design was developed with the objective to provide a simplified, user-friendly, and versatile device for collecting nanomechanical measurements associated with microbial activity in a wide range of growth media. The fundamental design components of the NMD consist of a light source, a sample chamber with an AFM cantilever mounting stage that facilitates light-cantilever-detector alignment, and a four-quadrant photodiode detector (QPD) (Figs. 1a and b).

The light source is a 650 nm Super Luminescent Emitting Diode (SLD, Exalos AG, Switzerland, Cat. No. EXS210030-03) that is focused using a fixed focal depth condenser (50 mm, Schäfer+Kirchhoff GmbH, Germany). The SLD provides a focused beam of light while reducing the risk of harmful exposure to more intense laser light sources often used in AFM instrumentation. The SLD is introduced into the NMD instrument via an optical fiber [22] where it then enters and exits the sample chamber with a 60 degree angle through sapphire windows that are

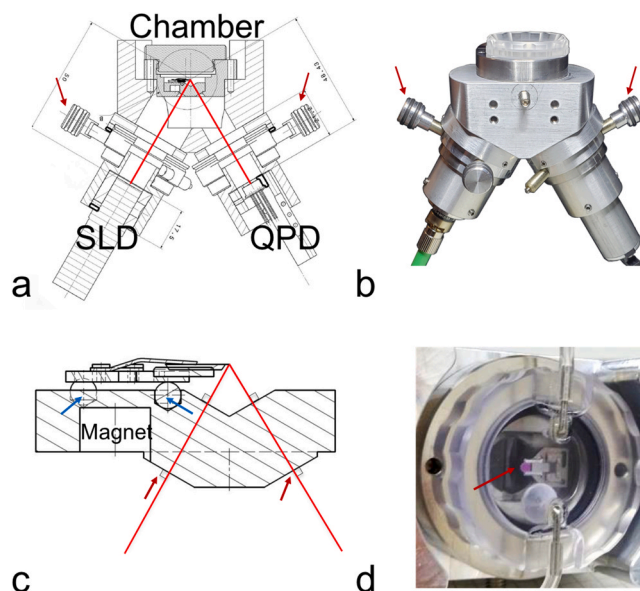


**Fig. 1.** The NMD design. a. Technical drawing in cutaway side-view showing where the SLD light path (red line) exits the condenser lens and is reflected by the cantilever onto the QPD. The red arrows indicate the fine X and Y axis alignment knobs for both the SLD and the QPD. Measurements are expressed in millimeters. b. A 3-D side view of the NMD (same orientation as (a)) with the sample chamber top screwed on. The red arrows indicate the fine alignment knobs in the X and Y axis. c. A side view of the sensor holder where the alignment setup is shown, including two of three total stainless-steel spheres (blue arrows) together with a magnet which allow the chip-holder to stay in position during NMD operation. The third sphere described in section “2.1” is hidden behind the left sphere in this depiction. The red arrows indicate where the two different sapphire windows enter the stainless-steel piece. d. The sample chamber sealed with a polycarbonate sample chamber cap that includes a sapphire window (to allow visibility of the inner chamber) and inlet and outlet ports for fluid exchange. A cantilever-bearing chip is mounted in the sample chamber (red arrow). (For interpretation of the references to color in this figure legend, the reader is referred to the web version of this article.)

in-line with the cantilever mounting system (Figs. 1a and c).

The sample chamber is a self-contained, stainless steel insert within the NMD that isolates aqueous reagents from the SLD and QPD electronics. The sample chamber reservoir holds up to 3 mL of liquid (e.g. growth media, Fig. 1a and d). This small reservoir volume minimizes the amount of time required for the sample chamber fluid, cantilever, and microbial sample to thermally equilibrate at the target temperature. The small volume also supports rapid mixing within the sample chamber when adding reagents or exchanging the chamber fluid using gravity or a rate-controlled pump. The exchange volume was determined empirically by monitoring the salinity during a fluid exchange between a saline to a freshwater solution to be approximately 3x the total volume for complete exchange. The stainless-steel sample chamber insert contains two sapphire windows that allow the SLD light path to enter the sample chamber, reflect off a cantilever within the chamber, and exit the chamber to the QPD (Fig. 1c). A threaded cap constructed of polycarbonate is fitted with a 200  $\mu\text{m}$  thick and 1 cm diameter sapphire window (Edmund Optics Ltd., York, UK) that allows users to align the SLD with the cantilever and observe microbes adhered to the cantilever via optical microscopy. Liquid exchange is achieved through stainless-steel inlet and outlet tubes (0.5 mm diameter, Fig. 1d) connected to a syringe or optional syringe pump (NE-1000 syringe pump, New Era Pump System Inc, USA) by silicon tubing.

The NMD sample chamber includes a two-component cantilever alignment system to simplify and improve the repeatability of the SLD-Cantilever-QPD alignment process. The first alignment component includes a three-node, magnetic mounting system that secures the

cantilever holder in the sample chamber on three stainless steel sphere-mounts (Fig. 1c). The second component of the alignment system uses an alignment chip (Alignment chips, Nanosensors GmbH, Germany) mounted in the cantilever holder to reliably insert the cantilever into the holder and thus enable reproducible micron-scale precision across experiments in which different cantilevers are used (Fig. 1d).

Users align the SLD-cantilever-QPD light path after mounting the cantilever in the sample chamber. This is achieved by turning the fine-scale manual X and Y adjustment knobs on both the SLD and QPD mounts. First, the light path is directed at the cantilever tip and confirmed via optical microscopy. Optimal light path alignment is achieved when the SLD beam is centered on the QPD. This is achieved by adjusting the manual X and Y fine-scale adjustment knobs on both the SLD and QPD in order to maximize the total QPD voltage signal and minimize signal offset from the center of the detector. The manual adjustment knobs allow users to optimize the QPD voltage signal and alignment to the hundredths place or better. A previous version of the NMD utilized small motors to enable remote, fine-scale SLD and QPD alignment. These motors, however, introduced a substantial amount of signal drift. The manual alignment knobs simplify the NMD, reduce signal drift from motor creep, and lower the NMD cost while still providing adjustable and stable light path alignment.

After entering the sample chamber, the aligned light path reflects off the cantilever and passes through the sapphire exit window where it illuminates the center of the QPD. The SLD-cantilever-QPD configuration and the angle of incidence renders the system independent of the refractive index of the growth medium inside the sample chamber. As the cantilever oscillates its motion is recorded via the concomitant transverse movement of the SLD light path across the QPD. The cantilever oscillations detected by the QPD are sent to a signal pre-amplifier and forwarded to an analog-to-digital converter card (National Instruments, Austin, TX, USA) that sends the data through an USB port to a computer running Labview (v 2017; National Instrument, Austin, TX, USA).

The NMD can accept traditional or tip-less cantilevers. Tip-less cantilevers (SD-qc-CONT-TL, Nanosensors GmbH, Germany) with a nominal spring constant of 0.1 N/m (Fig. 2a) are preferred since the tip does not interfere with cell attachment. The nominal spring constant is a key parameter to consider when selecting a cantilever since it impacts the signal to noise ratio. Furthermore, these tip-less cantilevers are partially gold coated with 20% coverage at the tip end of the cantilever that improves reflectivity of the SLD (Fig. 2a) and results in a significant reduction in  $1/f$  noise. Schumacher and colleagues demonstrated a greater Q-factor of partially-coated cantilevers that resulted in an increase of the sensitivity. Gold coating only at the tip of the cantilever also renders the signal less susceptible to drift due to thermal deltas [26].

Two NMD systems with slight differences in accessory and component configurations (e.g. optical microscope, vibration isolation, thermal control) were assembled and tested. One was used for AST assays at EPFL, and the other was employed at Desert Research Institute (DRI, Nevada, USA) for use in environmental microbiology research. Both NMD systems were mounted on vibration isolation tables to reduce signal contamination by external vibration sources such as user activities and building noise. SLD focal depth adjustments and SLD-cantilever alignment are achieved using long working distance light microscopes. The light microscopes also allow the user to observe microorganisms adhered to the cantilever over the duration of the experiment. The NMD used to collect the *E. coli* and *S. aureus* AST data at EPFL was mounted on a passive vibration isolation table (Technical Manufacturing Corporation, MA, USA) under a self-assembled transmitted-light microscope (Mitutoyo Corporation, Kawasaki, Kanagawa, Japan) with three ultralong working distance objectives providing 50–200 $\times$  magnification (Mitutoyo Infinity-Corrected Long Working Distance Objectives 5 $\times$ , 10 $\times$ , 20 $\times$ , Edmund Optics, York, UK). The NMD used in temperature-controlled nanomotion experiments at DRI was mounted on an active

vibration table (Accurion Nano30, Accurion GmbH, Göttingen, Germany) under a high-resolution digital microscope/camera with a 72 mm fixed working distance (UB503-LHK, Dunwell Tech. Inc., CA, USA). The NMD, vibration isolation table, and microscope were operated inside a Peltier-cooled/heated incubator (IPP 260 Plus, Memmert GmbH, Büchenbach, Germany) to control the temperature inside the NMD sample chamber. The Peltier-cooled incubator is highly preferable to traditional compressor-driven refrigeration systems due to vibrations that can affect the background signal and introduce signal noise. The DRI instrumentation platform is depicted in Fig. 3a.

## 2.2. NMD data acquisition

The data acquisition software was developed in Labview (National Instrument, TX, USA) at EPFL. This program processes and saves data coded at 16-bits in a one-dimensional array text file with a user-chosen rate that is at least double the cantilever resonant frequency. The program is available upon request. The data collection rate is typically acquired at 20 kHz for the tip-less SD-qc-CONT-TL cantilever that has a resonant frequency of  $\sim 8$  kHz in liquids. The software simultaneously records four measurements according to the incidence of the SLD light path on the QPD, including: (1) the SLD intensity or the total signal across the QPD, termed the SUM signal; (2) the vertical deflection of the cantilever, referred to as the deflection or DEF signal; (3) the lateral displacement of the cantilever, called the LFM signal; and (4) the DEF signal normalized by the SUM signal, named DEF/SUM.

Cellular activity is assessed based on the vertical deflection of the cantilever, or DEF signal, as described previously [29]. Briefly, deflection data are exported from Labview and post-processed in MATLAB to extract the cellular activity signal. The first post-processing step filters the signal with a low-pass filter to remove high frequency data. Thermal drift is then removed via best-fit linear flattening over 10 s bins. The variance of each 10 s bin is then calculated. Variance data is plotted as a function of time or further binned and plotted to show the variance median and standard deviation over desired (e.g. hour) timeframes. Variance data within box and whisker plots (Fig. 2d) are binned over 1 h ( $n=360$ ).

## 2.3. *E. coli* and cantilever preparation

*E. coli* (DH5<sup>TM</sup>, catalog Number: 18265017, Thermo Fisher Scientific, USA) was used at EPFL and strain K-12 at DRI) was cultured in Luria Broth (LB) medium at 37 °C on an orbital shaker. Similar experiments were also performed with *S. aureus* (see Supplementary information). Exponential phase cultures were rinsed three times in phosphate-buffered saline (PBS) by vortexing and subsequently centrifuged at 5000 rcf. Cells were then loaded on the cantilever as previously described ([29]). Briefly, cantilevers were functionalized with glutaraldehyde by immersing the cantilever in a droplet of 0.5% glutaraldehyde for 10 min, rinsing off the excess solution with 3 mL of ultra-pure water (resistivity: 18 M ohm  $\text{cm}^{-1}$ ), and allowing the cantilever to dry for 5 min in a laminar flow hood at room temperature. Washed *E. coli* cell pellets were diluted with 50–150  $\mu\text{L}$  of PBS to a final concentration of approximately  $5 \times 10^8$  cells per mL, based on optical density ( $\text{OD}_{600}=0.65$ ) spectrometer absorbance. The cells were adhered to the functionalized cantilever by incubating a 10  $\mu\text{L}$  droplet of the cell suspension on the cantilever for 30 min. Excess and poorly adhered cells were gently rinsed off the cantilever with 3 mL of LB and the cantilever was placed inside the NMD sample chamber. The binding agent used may vary based on microorganism external characteristics (cell wall/membrane, lipo-polysaccharides matrix, etc.). Several different binding compounds can be utilized, such as poly-L-lysine, glutaraldehyde, commercially available cell-tack and cationic polymers as presented in our previous work [29].

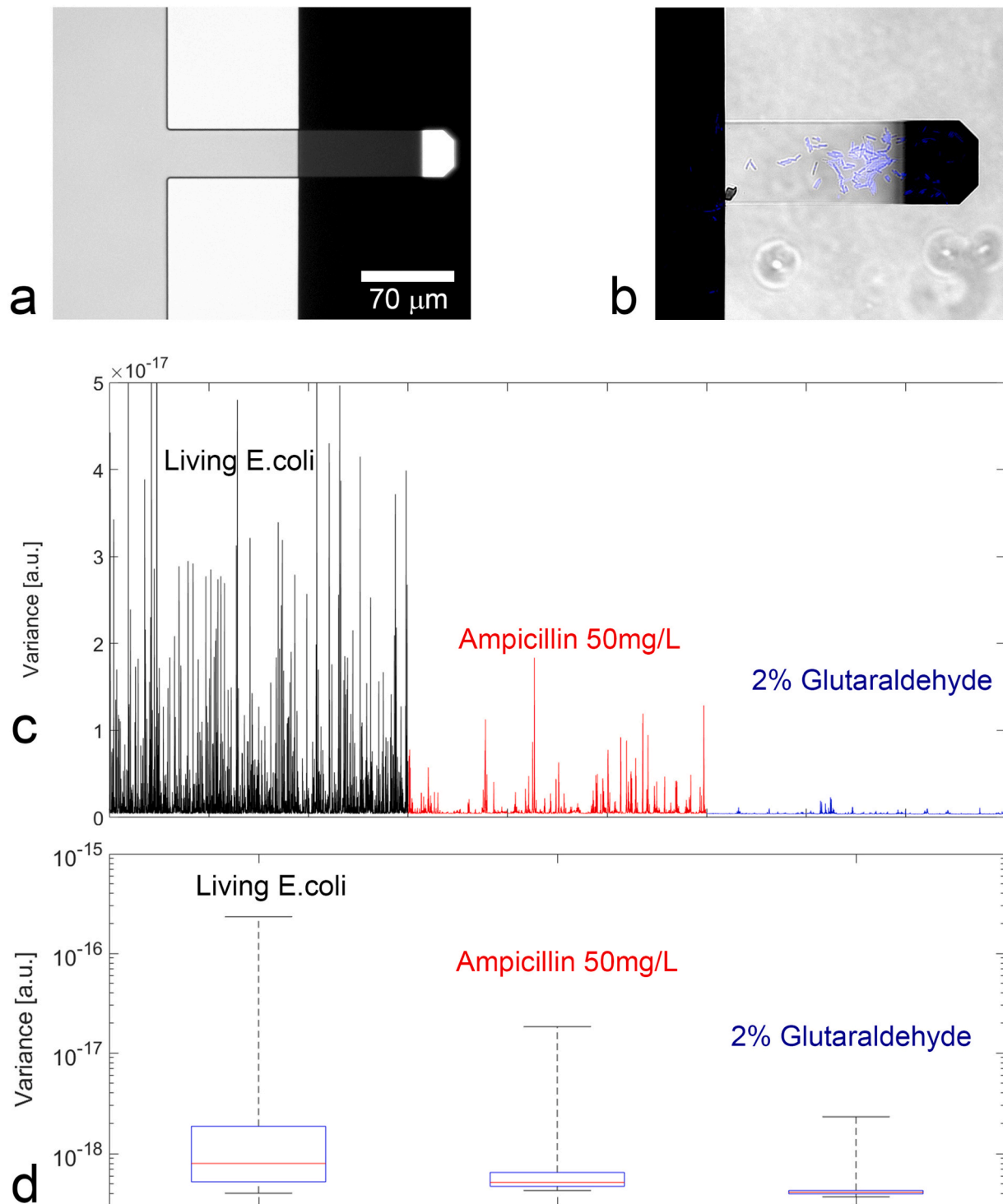
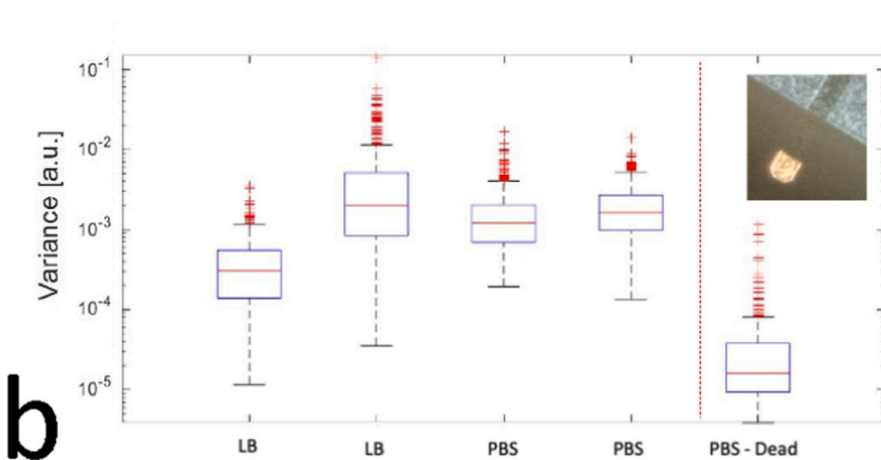


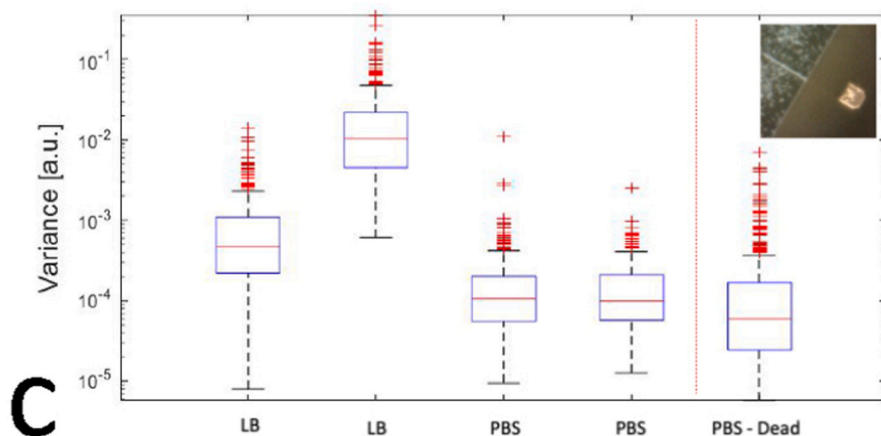
**Fig. 2.** A typical AST experiment using the NMD. a. A conventional commercially available tip-less AFM cantilever before functionalization and bacterial adhesion. b. The same cantilever with adhered, DAPI stained *E. coli* (blue cells). c. The variance of the cantilever deflection signal for each of the three incubation conditions determined for 1 h per treatment: LB (black line), antibiotic treatment (red line), and 2% glutaraldehyde (blue line). The number of fluctuations induced by the living organisms strongly reduce both in numbers and amplitude after the antibiotic injection. The signal measured after glutaraldehyde injection (blue line) is smaller than the antibiotic treatment signal highlighting the efficacy of glutaraldehyde for *E. coli* inactivation. These killed-control data are considered the system baseline. d. Deflection signal variance from c plotted as box and whisker plots (25th and 75th percentiles are shown together with the median value and the outliers (maximum and minimum values). Each box summarizes 1 h of data. (For interpretation of the references to color in this figure legend, the reader is referred to the web version of this article.).



a



b



c

**Fig. 3.** *E. coli* nanomotion was measured at 23 °C and at 30 °C inside a temperature-controlled incubator. a. The NMD device was operated inside the Peltier temperature-controlled incubator together with a vibration isolation table and digital microscope. b. *E. coli* cell nanomotion was measured at 23 °C for 2 h in LB medium prior to exchange LB with isotonic buffer for two hours (PBS: no carbon source), this was then followed by inactivation with glutaraldehyde (PBS-Dead) for one hour. The boxes defined by 25th and 75th quartiles (outliers shown in red), represent 1-hour data bins. c. *E. coli* cells analyzed at 30 °C in LB, PBS and after inactivation with glutaraldehyde (PBS-Dead). Plot representation is the same as in (b). Given variability between different cantilevers and cell loads, the data in b and c are not comparable. (For interpretation of the references to color in this figure legend, the reader is referred to the web version of this article.)

#### 2.4. ASTs and temperature-controlled cell activity experiments

AST experiments were conducted at EPFL with adhered *E. coli* or *S. aureus*. The sample chamber was filled with thermally equilibrated, filter sterilized (0.2  $\mu\text{m}$ ) LB. The cantilever and fluid were allowed to

equilibrate for 5–10 min prior to collecting data in order to reach a steady state and reduce signal drift. Each experiment was repeated in triplicate. Each experiment included three measurement phases: (1) live cells in LB (1 h); (2) exposure to either 150  $\mu\text{M}$  ampicillin in PBS (antibiotic treatment) or PBS (control, 1 h); and (3) treatment with 2%

glutaraldehyde (inactivation/killed control, 1 h). Liquid exchanges were performed using 10 mL of solution, which is approximately three times the total sample chamber volume (approximately 3 mL), in order to flush and replace the previous solution. The nanomotion data collection was stopped during the liquid exchange, in order to avoid recording a noise-induced signal by turbulence generated during the liquid exchange. Cells were inactivated by a final 2% glutaraldehyde treatment, stained with DAPI and observed at 630 $\times$  on a Zeiss Axiovert T-100 (typical example of cells attached on the cantilever is reported in Fig. 2b and Supplementary Fig. 2 c).

Changes in *E. coli* activity associated with growth media (LB vs. PBS) at two temperatures (23 °C and at 30 °C) were measured at DRI on a single NMD instrument located inside the Memmert IPP 260 Plus Peltier-controlled incubator. Cantilever-mounted cells were exposed to the following treatments and incubation durations in sequence: (1) LB growth medium (2 h); (2) PBS (2 h); (3) 2% glutaraldehyde (1 h). The system was allowed to equilibrate for 15–30 min between each treatment prior to collecting data concurrent with each incubation condition.

### 3. Experimental results and discussion

#### 3.1. Optimized NMD design

The NMD is a novel device designed specifically for measuring cell activity on a nanometric scale using commercially available AFM cantilevers. This device was optimized for the purpose of nanomotion detection, and ultimately negates the need to perform these measurements on AFMs, which are more expensive, complex, and prone to damage compared to the compact, functionally and operationally streamlined NMD. In particular, the NMD bears a range of features including a sealed sample chamber that supports fluid exchanges during an experiment, manual SLD and QPD alignment knobs, and a direct SLD-cantilever-QPD light path (Fig. 1a and b), all of which contribute to its robust, compact, and low-cost design. The SLD-cantilever-QPD light path eliminates the need for mirrors and mirror positioning systems that can be costly and have the potential to introduce signal drift and noise. Indeed, eliminating mirrors from earlier NMD designs and replacing a class 3 laser with an SLD light source reduced signal drift, increased the signal to noise ratio, and effectively increased the dynamic range of the instrument. Baseline or blank NMD nanomotion data recorded with a cantilever without any organisms attached onto its surface (data not shown) is two orders of magnitude lower than the signal observed for a typical *E. coli* sample.

#### 3.2. AST applications

We tested the NMD for its ability to rapidly perform ASTs using ampicillin against *E. coli* and ciprofloxacin against *S. aureus*. Using glutaraldehyde applied in a monolayer as an adhesion-agent consistently resulted in the adhesion of live *E. coli* cells onto the cantilever at concentrations sufficient to detect cellular nanomotion and therefore activity above inactivated cells. This is evidenced by the overall larger signal variance measured at the start of each experiment when cells are exposed to growth media, followed by a decrease in the magnitude of the variance after adding the antibiotic or glutaraldehyde (Figs. 2c,d, 3b,c). Signal variance as a function of time exhibits large fluctuations under all tested conditions, especially during live cell treatments (e.g. growth media) likely due to fluctuations in cell activity over time as well as their spatial distribution across the cantilever. It can be assumed that the signal contribution of any single cell will depend on its expressed activity, or nanomotion, and its location on the cantilever, and that the total signal is a combination of the contribution of each cell. Thus, many of the large fluctuations in variance are not necessarily anomalous data but rather indicate the collective range of combined activity for those cells based on the experimental conditions (e.g. number and location of cells, temperature and growth media), and likely indicate high activity

events.

While the measured variance may fluctuate over time and vary between each experimental run it is apparent that *E. coli* (or *S. aureus*) cells are inactivated by both antibiotics and glutaraldehyde based on the decrease in signal variance relative to the initial live-cell signal. As expected, the variance data indicate that antibiotics have less of an impact on cellular activity compared to the terminal effect of glutaraldehyde (Fig. 2c and d). It is also notable that the NMD signal is sufficiently sensitive to reveal that *E. coli* (or *S. aureus*) is more active following treatment by the antibiotic relative to the glutaraldehyde treatment.

Previous work using a different bacterial strain showed that an antibiotic treatment is often characterized by a lag in the nanomotion pattern followed by a partial reactivation after one hour [23]. This observation may have two explanations: (1) The presence of cells less susceptible to the antibiotic compared to the majority of the population; or (2) Cell activity is reduced upon antibiotic exposure but is later able to reactivate. The latter explanation is not supported by biological data. Regardless of the cause, the nanomotion signal that results from antibiotic treatment is unable to provide true Killed-control baseline data for which to compare live and treated nanomotion signals in any given nanomotion detection experiment. Glutaraldehyde treatment is therefore used to acquire the system baseline (killed-control) since it is an extremely effective killing agent and is assumed to terminate all cellular activity.

Quantifying DAPI-stained cells adhered to the cantilever provides an assessment of the NMD detection limit (Fig. 2b). A low amount of *E. coli* cells per cantilever (100) provided high quality nanomotion data with sufficient activity to exhibit statistically different variance signals between live, antibiotic-treated, and glutaraldehyde-killed conditions (Fig. 2c and d and Supplementary Fig. 1). The cell adhesion methods described herein, however, consistently resulted in sufficient *E. coli* cell adhesion onto the cantilever to enable positive AST results.

For the sake of comparison, *Staphylococcus aureus*, a non-motile bacteria, was tested in order to assess the independence of nanomotion measurement to cellular motility. Recording *S. aureus* before and after ciprofloxacin treatment showed a decrease in the nanomotion fluctuation confirming the capability of nano-fabricated sensors to identify the antibiotic susceptibility regardless of the presence of cellular flagella, pili or other motor-type organelles on the external surface of the microorganism (Supplementary Fig. 2).

More work is required to constrain the NMD detection limit, which will likely vary as a function of the experimental conditions tested, including but not limited to microbial species, experimental temperature, growth media, position of the cells on the cantilever in a given experiment. The cantilever type, including its geometry, spring constant, material, and reflectivity, also influence the analytical sensitivity.

#### 3.3. Effect of media and thermal control

Temperature plays a large role in bacterial metabolism and growth rate. Indeed, microbes are often categorized as meso-, thermo-, or psychrophiles depending on their optimal growth temperatures. Cells exhibit a range of growth rates and may even enter a maintenance metabolism state or undergo cell death when exposed to temperatures above or below their optimal growth conditions. The thermal tolerance range of a cell is dependent on its physiology and ability to adapt. It follows that experimental temperature control is crucial to understanding the activity of a cell and its response to antibiotics or other inactivation reagents.

Operating the NMD within a traditional compressor-driven incubator generated excessive external vibration that increased background noise and prevented collecting reliable nanomotion data. An active vibration table was unable to eliminate the signal noise from the incubator compressor. The vibrations from a traditional compressor-driven low-temperature incubator may be too large to compensate for given that the NMD is highly sensitive and able to measure forces on the order of pico-

Newtons. We expanded the versatility of the NMD by testing its ability to detect *E. coli* cell stress and inactivation within a Memmert IPP 260 Plus incubator. This incubator cools and heats using thermoelectric (Peltier) elements coupled with a low vibration fan. Ambient incubator vibrations are sufficiently dampened by the Nano30 active vibration isolation table to allow for high quality nanomotion data collection (Fig. 3).

*E. coli* activity measured at 23 °C (ambient room temperature) and 30 °C in LB resulted in an increase in nanometric cantilever oscillations over the course of two-hour incubations (Figs. 3b and 3c). The data are skewed towards high variance values which may denote “high activity” or large nanomotion events recorded by the NMD. The median NMD signal increased to a greater degree between the first and second hours at 30 °C compared to 23 °C (Fig. 3b, c). The 1-hour boxplot bins generally consistent with the doubling rate of *E. coli* at these temperatures [17], and the corresponding increase in signal activity suggests active *E. coli* growth and replication on the cantilever. *E. coli* nanomotion variance decreases within 30 min of adding PBS, suggesting a change in their cell activity. The observed *E. coli* nanomotion signal in PBS also remains steady over two hours incubation, indicating that cell replication may have slowed or even ceased (Fig. 3c). This behavior is anticipated given that PBS does not provide carbon or nutrient sources necessary to support heterotrophic growth. Treating the cells with a 2% glutaraldehyde solution kills the cells and results in an anticipated, concomitant decrease in nanomotion that is synonymous with the system baseline, or killed-control signal. These data indicate that *E. coli* nanomotion is detectable under both active (LB) and sub-optimal (PBS) incubation conditions relative to inactivated (killed) cells at 23 °C. Data at 30 °C suggest that *E. coli* cell activity was negligible in PBS and similar to activity, or the lack thereof, in the Glutaraldehyde killed-control. More work is required to constrain this result and understand the impacts of rapid nutrient loss on cell activity.

#### 4. Conclusions

In this study we present a novel nanomotion detector design (NMD) that enables rapid AST and live (active) cell detection studies under temperature-controlled conditions. The NMD exhibits a high signal to noise ratio that can distinguish between live, antibiotic-responsive, stressed, and inactivated-cell states with as few as 100 cells adhered to a commercially available, AFM cantilever. The NMD is also a robust, reliable, sensitive user-friendly instrument for medical and research laboratory applications that require in-house testing capabilities with living cells regardless of cellular motility. The streamlined design and low cost-fabrication affords experimental devices that can be operated in thermally controlled incubators which adds control and reproducibility. This paves the way for nanomotion applications to include large scale, rapid, and sensitive antibiotic susceptibility testing. The NMD can also support a wide range of microbial activity studies to support environmental or astrobiology research that explores complex environmental samples from aquatic, terrestrial, or icy environments and would benefit from an agnostic, or unbiased form of microbial activity detection.

#### CRedit authorship contribution statement

**LV:** Conceptualization, Methodology, Software, Validation, Formal analysis, Investigation, Data curation, Writing – original draft, Writing – review & editing, Visualization. **RF:** Conceptualization, Software, Formal analysis, Investigation, Writing – review & editing, Visualization, Project administration. **GD:** Conceptualization, Software, Resources, Writing – review & editing, Visualization, Supervision, Funding acquisition. **SK:** Conceptualization, Resources, Writing – review & editing, Visualization, Supervision, Funding acquisition. **ZRH:** Software, Validation, Formal analysis, Investigation, Writing – review & editing, Visualization. **MIV:** Investigation, Writing – review & editing, Visualization. **EML:** Writing – review & editing. **AEM:** Resources, Writing –

review & editing, Visualization, Supervision, Funding acquisition.

#### Declaration of Competing Interest

The authors declare the following financial interests/personal relationships which may be considered as potential competing interests: Sandor Kasas and Giovanni Dietler have patent #WO 2013/054311 A1 issued to EPFL.

#### Acknowledgments

This work was supported by the Swiss National Grants 200021-144321, 407240\_167137, CRSII5\_173863, the Gebert Rűf Stiftung GRS-024/14 and NASA-CLDTCH NNH16ZDA001N (USA).

#### Appendix A. Supporting information

Supplementary data associated with this article can be found in the online version at doi:10.1016/j.snb.2021.130650.

#### References

- [1] A.J. Alanis, Resistance to antibiotics: are we in the post-antibiotic era? Arch. Med. Res. 36 (2005) 697–705, <https://doi.org/10.1016/j.arcmed.2005.06.009>.
- [2] D. Alsteens, Y.F. Dufrẽne, Biophysics: rapid mass changes measured in cells, Nature 550 (2017) 465–466, <https://doi.org/10.1038/550465a>.
- [3] J. Barenfanger, C. Drake, G. Kacich, Clinical and financial benefits of rapid bacterial identification and antimicrobial susceptibility testing, J. Clin. Microbiol. 37 (1999) 1415–1418, <https://doi.org/10.1128/JCM.37.5.1415-1418.1999>.
- [4] S.J. Braunschweig, D. McIntosh, E. Vorotnikova, T. Zhou, K.A. Marx, Detection of apoptosis and drug resistance of human breast cancer cells to taxane treatments using quartz crystal microbalance biosensor technology, Assay. Drug Dev. Technol. 3 (2005) 77–88, <https://doi.org/10.1089/adt.2005.3.77>.
- [5] T.P. Burg, M. Godin, S.M. Knudsen, W. Shen, G. Carlson, J.S. Foster, K. Babcock, S. R. Manalis, Weighing of biomolecules, single cells and single nanoparticles in fluid, Nature 446 (2007) 1066–1069, <https://doi.org/10.1038/nature05741>.
- [6] M. Calleja, P.M. Kosaka, A. San Paulo, J. Tamayo, Challenges for nanomechanical sensors in biological detection, Nanoscale 4 (2012) 4925–4938, <https://doi.org/10.1039/c2nr31102j>.
- [7] N. Cermak, S. Olcum, F.F. Delgado, S.C. Wasserman, K.R. Payer, M.A. Murakami, S. M. Knudsen, R.J. Kimmerling, M.M. Stevens, Y. Kikuchi, A. Sandikci, M. Ogawa, V. Agache, F. Baleras, D.M. Weinstock, S.R. Manalis, High-throughput measurement of single-cell growth rates using serial microfluidic mass sensor arrays, Nat. Biotechnol. 34 (2016) 1052–1059, <https://doi.org/10.1038/nbt.3666>.
- [8] R. Daniels, Surviving the first hours in sepsis: getting the basics right (an intensivist’s perspective), J. Antimicrob. Chemother. 66 (2011) ii11–ii23, <https://doi.org/10.1093/jac/dkq515>.
- [9] R.T. Horvat, Review of antibiogram preparation and susceptibility testing systems, Hosp. Pharm. 45 (2010) 6–9, <https://doi.org/10.1310/hpj4511-s6>.
- [10] W.L. Johnson, D.C. France, N.S. Rentz, W.T. Cordell, F.L. Walls, Sensing bacterial vibrations and early response to antibiotics with phase noise of a resonant crystal, Sci. Rep. 7 (2017) 12138, <https://doi.org/10.1038/s41598-017-12063-6>.
- [11] S. Kasas, A. Malovichko, M.I. Villalba, M.E. Vela, O. Yantorno, R.G. Willaert, Nanomotion detection-based rapid antibiotic susceptibility testing, Antibiot. (Basel, Switz.) 10 (2021) 287, <https://doi.org/10.3390/antibiotics10030287>.
- [12] S. Kasas, F.S. Ruggeri, C. Benadiba, C. Maillard, P. Stupar, H. Tournu, G. Dietler, G. Longo, Detecting nanoscale vibrations as signature of life, Proc. Nat. Acad. Sci. U.S.A. 112 (2015) 378–381, <https://doi.org/10.1073/pnas.1415348112>.
- [13] A.-C. Kohler, L. Venturelli, A. Kannan, D. Sanglard, G. Dietler, R. Willaert, S. Kasas, Yeast nanometric scale oscillations highlights fibronectin induced changes in *C. albicans*, Fermentation 6 (2020) 28, <https://doi.org/10.3390/fermentation6010028>.
- [14] A.C. Kohler, L. Venturelli, G. Longo, G. Dietler, S. Kasas, Nanomotion detection based on atomic force microscopy cantilevers, Cell Surf. 5 (2019), 100021, <https://doi.org/10.1016/j.tcs.2019.100021>.
- [15] M. Krieg, G. Fläschner, D. Alsteens, B.M. Gaub, W.H. Roos, G.J.L. Wuite, H.E. Gaub, C. Gerber, Y.F. Dufrẽne, D.J. Müller, Atomic force microscopy-based mechanobiology, Nat. Rev. Phys. 1 (2018) 41–57, <https://doi.org/10.1038/s42254-018-0001-7>.
- [16] F. Lang, G.L. Busch, M. Ritter, H. Völkl, S. Waldegger, E. Gulbins, D. Häussinger, Functional significance of cell volume regulatory mechanisms, Physiol. Rev. 78 (1998) 247–306, <https://doi.org/10.1152/physrev.1998.78.1.247>.
- [17] C. Lissandrello, F. Inci, M. Francom, M.R. Paul, U. Demirci, K.L. Ekinci, Nanomechanical motion of *Escherichia coli* adhered to a surface, Appl. Phys. Lett. 105 (2014), 113701, <https://doi.org/10.1063/1.4895132>.
- [18] A.C. Lloyd, The regulation of cell size, Cell 154 (2013) 1194–1205, <https://doi.org/10.1016/j.cell.2013.08.053>.
- [19] G. Longo, L. Alonso-Sarduy, L.M. Rio, A. Bizzini, A. Trampuz, J. Notz, G. Dietler, S. Kasas, Rapid detection of bacterial resistance to antibiotics using AFM

- cantilevers as nanomechanical sensors, *Nat. Nanotechnol.* 8 (2013) 522–526, <https://doi.org/10.1038/nnano.2013.120>.
- [20] N.F. Martínez, P.M. Kosaka, J. Tamayo, J. Ramírez, O. Ahumada, J. Mertens, T. D. Hien, C.V. Rijn, M. Calleja, High throughput optical readout of dense arrays of nanomechanical systems for sensing applications, *Rev. Sci. Instrum.* 81 (2010), 125109, <https://doi.org/10.1063/1.3525090>.
- [21] D. Martínez-Martín, G. Fläschner, B. Gaub, S. Martin, R. Newton, C. Beerli, J. Mercer, C. Gerber, D.J. Müller, Inertial picobalance reveals fast mass fluctuations in mammalian cells, *Nature* 550 (2017) 500–505, <https://doi.org/10.1038/nature24288>.
- [22] G. Meyer, N.M. Amer, Novel optical approach to atomic force microscopy, *Appl. Phys. Lett.* 53 (1988) 1045–1047, <https://doi.org/10.1063/1.100061>.
- [23] A. Mustazzolu, L. Venturelli, S. Dinarelli, K. Brown, R.A. Floto, G. Dietler, L. Fattorini, S. Kasas, M. Girasole, G. Longo, A rapid unravelling of mycobacterial activity and of their susceptibility to antibiotics, e02194-18, *Antimicrob. Agents Chemother.* 63 (2019), <https://doi.org/10.1128/AAC.02194-18>.
- [24] L. Nowacki, J. Follet, M. Vayssade, P. Vigneron, L. Rotellini, F. Cambay, C. Egles, C. Rossi, Real-time QCM-D monitoring of cancer cell death early events in a dynamic context, *Biosens. Bioelectron.* 64 (2015) 469–476, <https://doi.org/10.1016/j.bios.2014.09.065>.
- [25] F.S. Ruggeri, A.-L. Mahul-Mellier, S. Kasas, H.A. Lashuel, G. Longo, G. Dietler, Amyloid single-cell cytotoxicity assays by nanomotion detection, *Cell Death Discov.* 3 (2017) 17053, <https://doi.org/10.1038/cddiscovery.2017.53>.
- [26] Z. Schumacher, Y. Miyahara, L. Aeschmann, P. Grütter, Improved atomic force microscopy cantilever performance by partial reflective coating, *Beilstein J. Nanotechnol.* 6 (2015) 1450–1456, <https://doi.org/10.3762/bjnano.6.150>.
- [27] K. Syal, M. Mo, H. Yu, R. Iriya, W. Jing, S. Guodong, S. Wang, T.E. Grys, S. E. Haydel, N. Tao, Current and emerging techniques for antibiotic susceptibility tests, *Theranostics* 7 (2017) 1795–1805, <https://doi.org/10.7150/thno.19217>.
- [28] J. Tamayo, P.M. Kosaka, J.J. Ruz, Á. San Paulo, M. Calleja, Biosensors based on nanomechanical systems, *Chem. Soc. Rev.* 42 (2013) 1287–1311, <https://doi.org/10.1039/c2cs35293a>.
- [29] L. Venturelli, A.-C. Kohler, P. Stupar, M.I. Villalba, A. Kalauzi, K. Radotić, M. Bertacchi, S. Dinarelli, M. Girasole, M. Pešić, J. Banković, M.E. Vela, O. Yantorno, R. Willaert, G. Dietler, G. Longo, S. Kasas, A perspective view on the nanomotion detection of living organisms and its features, *J. Mol. Recognit.* 33 (2020) 2849, <https://doi.org/10.1002/jmr.2849>.
- [30] M.I. Villalba, L. Venturelli, R. Willaert, M.E. Vela, O. Yantorno, G. Dietler, G. Longo, S. Kasas, Nanomotion spectroscopy as a new approach to characterize bacterial virulence, *Microorganisms* 9 (2021) 1545, <https://doi.org/10.3390/microorganisms9081545>.
- [31] G. Wang, A.H. Dewilde, J. Zhang, A. Pal, M. Vashist, D. Bello, K.A. Marx, S. J. Braunhut, J.M. Therrien, A living cell quartz crystal microbalance biosensor for continuous monitoring of cytotoxic responses of macrophages to single-walled carbon nanotubes, *Part. Fibre Toxicol.* 8 (2011) 4, <https://doi.org/10.1186/1743-8977-8-4>.
- [32] R.G. Willaert, P. Vanden Boer, A. Malovichko, M. Alioscha-Perez, K. Radotić, D. Bartolić, A. Kalauzi, M.I. Villalba, D. Sanglard, G. Dietler, H. Sahli, S. Kasas, Single yeast cell nanomotions correlate with cellular activity, *Sci. Adv.* 6 (2020) 3139, <https://doi.org/10.1126/sciadv.aba3139>.
- [33] T.A. Zangle, M.A. Teitell, Live-cell mass profiling: an emerging approach in quantitative biophysics, *Nat. Methods* 11 (2014) 1221–1228, <https://doi.org/10.1038/nmeth.3175>.
- Leonardo Venturelli, PhD: postdoctoral research associate at the EPFL (Lausanne, Switzerland) from 2017 to 2020. His main interest pertains to the detection of life in the field of astrobiology.
- Zoë Harrold, PhD: Dr. Harrold, an Assistant Research Scientist at DRI (Reno, NV) from 2019 to 2020, now an independent consultant, is a geomicrobiologist with broad experience in environmental sampling, laboratory experimentation, and sample analysis.
- Alison E. Murray, PhD, Research Professor: Dr. Murray is a molecular microbial ecologist and biological oceanographer with research interests centered around a common theme of utilizing molecular biological and genomic approaches to describe the diversity of life, understand the evolutionary history, ecological roles, and physiological capacity and capabilities of free-living and symbiotic microorganisms several of which are considered to be at the extremes of where life exists.
- Maria Ines Villalba, PhD: Postdoc researcher at EPFL (Lausanne, Switzerland). Her interests and research span from microbial life detection to molecular biology and statistical interpretation of data.
- Eric Lundin, MS: researcher in biology with interests in microbial life detection, molecular biology, and mathematical applications to biology.
- Giovanni Dietler, PhD: full professor of Physics at the EPFL (Lausanne, Switzerland). Professor Dietler main research line is dedicated to the basic building blocks of living matter, namely proteins, DNA and cells. With this research we are investigating these molecules and cells as the fundamental building blocks of the living matter with the purpose of understanding the physical properties relevant to their function. Mechanical properties, interaction between proteins, statistical properties of DNA are measured by the Atomic Force Microscope or by other spectroscopic methods like local infrared absorption spectroscopy.
- Sandor Kasas, PhD, Scientist at the EPFL (Lausanne, Switzerland): Dr. Kasas' interests pertain the detection of living organisms from bacteria to mammalian cells using micro-metric and nanometric optical devices and AFM-based techniques.
- Raphael Foschia: scientist at the University of Applied Sciences and Arts Western Switzerland in Geneva. His research interest pertains mainly to the design and development of optical and scanning probes apparatus for the detection of microorganisms and surfaces properties measurements.